Source apportionment and dynamic changes of carbonaceous aerosols during the haze bloom-decay process in China based on radiocarbon and organic molecular tracers

Junwen Liu[1], Jun Li[1], Di Liu[1], Ping Ding[2], Chengde Shen[2], Yangzhi Mo[1], Xinming Wang[1], Chunling Luo[1], Zhineng Cheng[1], Sönke Szidat[3], Yanlin Zhang[3], Yingjun Chen[4], and Gan Zhang[1]

[1]State Key Laboratory of Organic Geochemistry, Guangzhou Institute of Geochemistry, Chinese Academy of Sciences, Guangzhou, 510640, China

[2]State Key Laboratory of Isotope Geochemistry, Guangzhou Institute of Geochemistry, Chinese Academy of Sciences, Guangzhou, 510640, China

[3]Department of Chemistry and Biochemistry & Oeschger Centre for Climate Change Research, University of Bern, Berne, 3012, Switzerland

[4]College of Environmental Science and Engineering, Tongji University, Shanghai, 200092, China

Correspondence to: Jun Li (junli@gig.ac.cn).

Abstract

Fine carbonaceous aerosols (CAs) is the key factor influencing the currently filthy air in megacities of China, yet seldom study simultaneously focuses on the origins of different CAs species using specific and powerful source tracers. Here, we present a detailed source apportionment for various CAs fractions, including organic carbon (OC), water-soluble OC (WSOC), water-insoluble OC (WIOC), elemental carbon (EC) and secondary OC (SOC) in the largest cities of North (Beijing, BJ) and South China (Guangzhou, GZ), respectively, using the measurements of radiocarbon and anhydrosugars. Results show that non-fossil fuel sources such as biomass burning and biogenic emission make a significant contribution to the total CAs in Chinese megacities: 56±4% in BJ and 46±5% in GZ, respectively. The relative contributions of primary fossil carbon from coal and liquid petroleum combustions, primary non-fossil carbon and secondary organic carbon (SOC) to total carbon are 19%, 28% and 54% in BJ, and 40%, 15% and 46% in GZ, respectively. Non-fossil fuel sources account for 52% in BJ and 71% in GZ of SOC, respectively. These results suggest that biomass burning has a greater influence on regional particulate air pollution in North China than in South China. We observed an unabridged haze bloom-decay process in South China, which illustrates that both primary and secondary matter from fossil sources played a key role in the blooming phase of the pollution episode, while haze phase is predominantly driven by fossil-derived secondary organic matter and nitrate.

1 Introduction

Particulate matter with an aerodynamic diameter of <2.5 μm ($PM_{2.5}$) is either directly emitted from emission sources (chemical industry, power plant, vehicle, biomass burning, soil dust, etc.) or formed as secondary particles via the conversion of volatile organic compounds (VOCs) and inorganic gases (SO_2/NO_X/NH_3) to the particulate phase. These tiny particles have been shown to cause numerous environmental, health and climate problems that closely link humans and the global climate system. (Brunekreef et al., 2002; Dockery et al., 1993; Huang et al., 2014a, Wang et al., 2011; Wang et al., 2014). Many countries or regions have set strict standards for the ambient concentration of $PM_{2.5}$ in an attempt to improve public health and protect air quality. For example, the annual and 24-hour $PM_{2.5}$ standards are regulated at 35 μg/m^3 and 75 μg/m^3, respectively, in China.

As the world's largest contributor of $PM_{2.5}$ (Huang et al., 2014b), China is currently facing the challenge of severe air pollution (i.e., haze episodes) (Chan et al., 2008; Zhang et al., 2012), which has already led to numerous negative impacts on the atmospheric environment and public health. Up to 1.2 million premature deaths in China were directly or indirectly correlated with air pollution in 2010 (Lim et al., 2013). Furthermore, haze events in Chinese urban areas, especially in megacities, have become a common phenomenon that can occur during any season owing to the intensive emissions of pollutants and unfavorable meteorological conditions (He et al., 2014; Liu et al., 2013a). Better understanding of $PM_{2.5}$ sources and formation processes, which remain unclear due to the complicated chemical constituents, is urgently needed and would greatly facilitate the development of steps to mitigate the serious haze pollution in China.

Carbonaceous aerosols (CAs) in $PM_{2.5}$ have been shown to be crucial factors in the haze episodes. In a highly polluted region, ~40% of $PM_{2.5}$ can be explained by CAs (Cao et al. 2003), exerting remarkable impacts on the atmospheric visibility (Deng et al. 2008). Traditionally, CAs, of which classification

approach is method-dependent, are categorized as organic carbon (OC) and elemental carbon (EC). OC represents the less refractory CAs that contain thousands of organic molecules either emitted by primary emission sources (primary organic carbon, POC) or formed by the conversion process of gas-to-particle (secondary organic carbon, SOC). In addition, OC also can be further classified into water-soluble organic carbon (WSOC) and water-insoluble organic carbon (WIOC). EC is formed only during incomplete combustion processes. TC is the sum of OC and EC. In recent years, source apportionments for these carbon species have yielded useful information in China through radiocarbon (^{14}C)-based top-down studies. At the early period, studies related the ^{14}C of atmospheric CAs were focusing on the TC fraction in China. It was reported that ~30-50% of $PM_{2.5}$ TC is contributed from modern/non-fossil sources in Beijing during the year of 2001 (Yang et al., 2005). In Lhasa, a remote city of China, non-fossil sources accounted ~for 36-70% of TC (Huang et al., 2010). In a background site of Southeast China, Niu et al. (2013) observed the obvious seasonality of percentages of non-fossil sources in TC: ~45% in summer and ~95% in winter, respectively. Nowadays, studies are beginning to concern the origins of sub-fractions of CAs, i.e., EC and OC in the filthy air of Chinese cities. Chen et al. (2013) first systematically studied the ^{14}C levels of EC, also known as black carbon, in East Asia and found that fossil-fuel combustion contributed 80±6% of the EC emitted from China, which is confirmed by the studies of Liu et al. (2014) and Zhang et al. (2015). Using the combined measurements of ^{14}C and stable carbon isotope (^{13}C), Andersson et al. (2015) further pointed out that the sources of EC covering China are highly region-specific, probably due to the big difference of energy consumption among regions. Concerning OC, Zhang et al. (2015) found that the averaged contribution of fossil sources is 35-58% in Chinese cities with the rest come from non-fossil sources such as biomass burning and biogenic emissions. Through combining a series of analytical methods with ^{14}C, Huang et al. (2014a) believed that haze enveloping Chinese cities are subject to secondary aerosols, which accounting for 30-77% of $PM_{2.5}$ and 41-71% of organic aerosols, respectively. However, most of

these studies have emphasized only the ^{14}C levels of one or two carbon species, and our understanding of haze formation remains limited. In this study, ^{14}C levels for the various carbon species (WIOC, WSOC, OC, EC, and TC) are reported simultaneously in two cities located in North and South China, respectively. To further constrain the atmospheric behavior of $PM_{2.5}$, secondary inorganic ions (SO_4^{2-}, NO_3^- and NH_4^+), primary inorganic ions (K^+, Ca^{2+}, Mg^{2+}, Cl^- and Na^+) and biomass burning-specific organic tracers (Simoneit et al. 2001) (levoglucosan, Lev; Galactosan, Gal; Mannosan, Mann) were also measured. Finally, a detailed source apportionment of CAs and $PM_{2.5}$ was achieved in the largest city of North (Beijing) and South China (Guangzhou) using the measurements of ^{14}C and other organic/inorganic chemicals, and the source dynamics of individual primary and secondary aerosols during the haze bloom-decay process in Guangzhou basing day-to-day time serials and Beijing basing low-to-high $PM_{2.5}$ concentrations were investigated as well.

2 Materials and Methods

2.1 Field Sampling Campaign

Twenty-four-hour $PM_{2.5}$ samples (9:00 a.m. to 9:00 a.m. the following day) were collected continuously on pre-baked quartz fiber filters (8×10 inches, Pall) through a high-volume sampler that equipped with a $PM_{2.5}$ inlet (1 m^3/min, XT Instruments, Shanghai, China) in China's two largest megacities, located in North (Beijing, BJ, 39.9°N, 116.4°E, ~20 million inhabitants; 21 samples) and South China (Guangzhou, GZ, 23.1°N, 113.3°E, ~10 million inhabitants; 14 samples) during March and April, 2013, respectively (Fig. 1). The meteorological parameters during sampling are shown in Fig. S1. After sampling, the filters were folded, wrapped in aluminum foil, sealed in airtight plastic bags, and stored in a refrigerator at -20 ℃ until analysis. Three field blanks were collected from both sampling sites.

2.2 Separation for Carbon Species

A punch of filter was cut and sandwiched by a filtration unit equipped with a quartz cartridge, and subsequently extracted by 100-mL ultra-pure water (18.2 MΩ) carefully. Only ~5% of carbon in original filter was lost during this water-extraction and thus the resulting bias towards the measurement of WIOC and EC and the source apportionment of TC in the following text is marginal and can be neglected. WSOC species were quantified using a TOC analyzer (Shimadzu TOC_VCPH, Japan). The washed filter was dried in a desiccator, wrapped in aluminum foil and stored in a refrigerator. Contribution of carbonate carbon (CC) to fine aerosols generally can be neglected if studies focusing on the CAs (Chow and Watson, 2002). While, some early investigations showed that CC-rich dusts derived from deserts may exert a substantial influence on the air quality during the spring season in North China (He, et al., 2001; Zheng, et al., 2005). Thus, hydrochloric acid (1 M) was used to remove the potential CC in the samples collected in BJ in this study. WIOC and EC were obtained from the water-filtered sample using an off-line carbon analyzer (Sunset Laboratory, Inc., US) by the thermo-optical transmittance method (NIOSH 870). The average WIOC contents in the field blanks from BJ and GZ were 0.25±0.02 μg/cm^2 and 0.26±0.03 μg/cm^2, respectively. No EC and WSOC were detected in any of the field blanks. In this study, the reproducibility of the measurement of WIOC, EC, and WSOC is 5%, 7%, and 9%, respectively (n=4).

2.3 Radiocarbon Measurements

Isolation procedures for the ^{14}C measurements of WIOC, EC and WSOC have been described previously (Liu et al., 2013b; Liu et al., 2014; Zhang et al. 2010a). In brief, WIOC and EC were combusted in a stream of pure oxygen at 340 ℃ for 15 min and 650 ℃ for 10 min, respectively. Prior to combustion at 650 ℃, EC was placed in a tube furnace at 375 ℃ for 4 h with air. WSOC solution was frozen, freeze-dried, and then combusted at 850 ℃. Graphite target preparations and accelerator mass spectrometry (AMS) measurements

were performed at the Guangzhou Institute of Geochemistry, Chinese Academic Sciences (GIGCAS) and Peking University NEC compact AMS facility, respectively. All ^{14}C values were reported as the fraction of modern carbon (f_m) after correction with $\delta^{13}C$ for fractionation. f_m was converted into the fraction of contemporary carbon (f_c) to eliminate the effect of nuclear bomb tests through conversion factors (Mohn et al., 2008), which were 1.10±0.05 for EC and 1.06±0.05 for OC in 2013 (Liu et al., 2014), respectively. Both f_c values for TC and OC were calculated by isotopic mass balance. No blank corrections were performed owing to the low carbon amount in the filed blanks in this study, which accounted for only <2% of samples.

2.4 Levoglucosan, Galactosan and Mannosan

Levoglucosan (Lev), Galactosan (Gal) and Mannosan (Mann) are regarded as excellent tracers for biomass burning activities (Simoneit et al. 2001). Detailed analytical procedure has been described in Liu et al. (2013b, 2014). In brief, a section of filter was removed, spiked with 500 ng of methyl-β-L-xylanopyranoside (m-XP) as internal standards, extracted with methanol, reduced using a rotary evaporator, filtered through a Teflon syringe filter, dried in a stream of gentle nitrogen, and then reacted with a mixture of 40-μL BSTFA (1% TMCS) and pyridine at 70 ℃ for 1 h. Subsequently, this derivatization solution was injected into a gas chromatograph-mass spectrometer (GC-MS, Agilent 7890-5975) with a capillary column (DB-5MS, 30 m, 0.25 mm, 0.25 μm).

2.5 Inorganic Ions

A 2.54 cm^2 filter was punched out, extracted twice in ultra-pure water (18.2 MΩ) with a centrifuge, sonicated in an ice-water bath, and filtrated using a Teflon syringe filter (0.22 μm). Subsequently, the filtrates were combined and analyzed for anions and ions (Na^+, Cl^-, Ca^{2+}, Mg^{2+}, K^+, NH_4^+, SO_4^{2-} and NO_3^-) using an ion chromatography (Metrohm 883 Basic IC plus, Switzerland). Small amounts of Mg^{2+}, Ca^{2+}, Cl^-

and SO_4^{2-} were detected in the field blanks, and their corresponding concentrations in samples were corrected. The other ions were not be detected in the field blank filters. The reproducibility of these ions ranged between 5% and 11% (n=4) in this study.

2.6 Methodology for the Source Apportionment of Carbons

2.6.1 The Separation of Fossil and Non-fossil Carbon Species

The concentrations of non-fossil/fossil carbon species were directly calculated using their corresponding f_c values as mentioned above. For example, the concentrations of fossil WIOC ($WIOC_f$) and non-fossil WIOC ($WIOC_{nf}$) were calculated as follows:

$$WIOC_f = (1- f_c(WIOC)) \times WIOC$$

$$WIOC_{nf} = f_c(WIOC) \times WIOC$$

Thus, all carbon species could be separated into non-fossil and fossil fractions. EC is formed directly by incomplete combustion processes, with non-fossil source EC emitted from biomass burning activities.

2.6.2 Primary Organic Carbon

OC particles exiting in the present atmosphere are actually a mixture of POC and SOC. POC is the sum of primary biomass burning OC (POC_{bb}), primary fossil fuel combustion-derived OC (POC_f) and the carbonaceous material that exists in vegetation debris, bioaerosols and resuspended soil organic matter. Since vegetation debris, bioaerosols and soil dust in the air is generally much larger than 2.5 μm, its portion in $PM_{2.5}$ is small and can be neglected, especially in highly polluted air. For example, it was reported that vegetation debris accounted for only ~1% of $PM_{2.5}$ OC in Beijing, China (Guo et al., 2012). Moreover, although soil dust may contribute to the primary inorganic aerosol at Beijing (Huang et al., 2014a), its impact on CAs is negligible due to the low carbon content of soil. Thus, this fraction of OC was ignored in

our study. The fraction of POC_{bb} can be estimated using the concentration of Lev, which is an excellent molecular marker for biomass burning, with the hypothesis that the POC_{bb}/Lev value is maintained at a stable level during transportation from emission sources to the ambient environment. In the real atmosphere, Lev is gradually oxidized and degraded (Hoffmann, et al., 2009). However, this decay occurs mainly in typical summer conditions, with 1×10^6 molecules cm^{-3} of hydroxyl radicals and independent of relative humidity, according to smog chamber results (Hennigan et al., 2010). Our study, however, was performed in spring with lower temperatures (lower hydroxyl radical levels), and air masses containing biomass burning-derived particles were derived mainly from the sub-urban/rural areas around the sampling locations (relatively shorter air transportation distances). Thus, it was appropriate to use Lev to estimate POC_{bb} in this study.

$$POC_{bb} = Lev \times (POC/Lev)_{bb}$$

$(POC/Lev)_{bb}$, the ratio of primary OC to Lev in the pure biomass burning particles, is closely related to the type of biomass burning (Fine et al., 2002). According to information from previously reported emission inventories, the mean values of $(POC/Lev)_{bb}$ for hardwood, softwood, and annual plants are 7.76, 14.2 and 13.5 with uncertainties of 19%, 22%, and 22%, respectively (Fig. S3).

OC directly emitted from fossil fuel combustion is, in principle, water-insoluble (Weber et al., 2007; Zhang et al., 2014). This was further confirmed in a recent study performed by Dai et al. (2015), who found >90% of traffic tunnel-emitted OC is water-insoluble, implying that primary fossil organic carbon (POC_f) should be nearly exclusively water-insoluble, if considering the limited but existing SOC in the traffic tunnel. Therefore, POC_f is estimated by the fraction of $WIOC_f$.

$$POC_f = WIOC \times (1- f_c(WIOC))$$

2.6.3 Secondary Organic Carbon

Non-fossil OC is composed of POC_{bb} and non-fossil SOC (SOC_{nf}) neglecting any contribution from plant debris. Thus, SOC_{nf} can be estimated as follows:

$$SOC_{nf} = OC_{nf} - POC_{bb}$$

It should be noted that the VOC precursors of SOC_{nf} can originate from both biogenic emissions and biomass burning.

Studies have found that fossil WSOC can serve as an accurate proxy for fossil SOC (SOC_f) (Liu et al., 2014; Zhang et al., 2014), which was therefore calculated by the following:

$$SOC_f = WSOC \times (1- f_c(WSOC))$$

Some fossil SOC may exist in water-insoluble phase. In Tokyo, Japan, Miyazaki et al. (2006) estimated that <30% of SOC is water-insoluble, mainly representing fresh SOC (Favet et al., 2008).. It is very likely that practically all SOC species would exist in water-soluble phases, if they underwent sufficient atmospheric reaction. Note that a small part of fresh SOC that exists in the water-insoluble phase is not taken into account for the estimation of fossil SOC, although samples were collected every 24 hours in this study.

3 Results and Discussion

3.1 $PM_{2.5}$ and Chemical Composition

Extremely high $PM_{2.5}$ mass concentrations are detected in both BJ (74.7–418 μg/m^3, mean 218 μg/m^3) and GZ (46.1–145 μg/m^3, mean 90.6 μg/m^3) (Fig. 1), compared to the Chinese first-grade air quality standard (35 μg/m^3, 24-hour) and the World Health Organization (25 μg/m^3, 24-hour). Such elevated $PM_{2.5}$ loadings can be vividly observed from space (Fig. S2). In this study, the average $PM_{2.5}$ concentration in BJ is 2.4-fold higher than that in GZ, indicating poorer air quality over the North China region, which has been found in previous investigations (Cao et al., 2012) and is also consistent with the fact that BJ and the adjacent suburban/rural areas (North China Plain) have the world's highest population density. Organic matter (OM)

is the largest contributor to $PM_{2.5}$ in both cities (Fig. 1), followed by NO_3^- (13%), SO_4^{2-} (9.5%), NH_4^+ (5.8%), Ca^{2+} (2.6%), Cl^- (2.6%), and EC (1.1%) in BJ and SO_4^{2-} (16%), NO_3^- (10%), NH_4^+ (7.6%), EC (3.2%), and Cl^- (2.0%) in GZ. OM calculations are based on the relative contributions of WSOC and WIOC in OC, due to the different conversion factors for WIOC to WIOM (1.3) and WSOC to WSOM (2.1) (Yttri et al., 2007; Favez et al. 2009; Sun et al. 2011; Chen et al. 2014). OM is the sum of WIOM and WSOM. The proportions of the other measured chemicals are generally lower than 1%. In this study, ~40-50% of $PM_{2.5}$ are unidentified, which is relatively higher than that (~10-36%) from a recent study performed in China (Huang et al. 2014a) and probably because we didn't measure elementals and their oxidants in $PM_{2.5}$. Fox example, Chen et al. (2001) found ~35-40% of $PM_{2.5}$ can't be identified in Taiwan without measuring some constituents such as Cu, Cd, and As. In addition, the water absorbed by organics would also influence the proportion of unidentified fraction in particles (Andrews et al. 2000). Different chemical compositions are largely reflective of their different source characteristics and the corresponding atmospheric processes. For example, the higher concentrations of Ca^{2+} recorded in BJ in this study are due to the extensive dust storms originating from deserts in northwestern regions that strongly impact North China in spring (He et al., 2001; Zheng et al., 2005). Road and construction fugitive dust also can lead to a relative high Ca^{2+} in $PM_{2.5}$, while this source may mainly influences Beijing in summer and is insignificant in spring (Zheng et al. 2005). In addition, biomass burning activities, using domestic biofuel, are generally more widespread in North China (Liu et al., 2007), which is reflected by the higher levels of biomass burning markers (Lev and K^+) in BJ (Table 1).

3.2 Radiocarbon Results

Although the chemical compositions of $PM_{2.5}$ can largely be identified by state-of-the-art analytical technology (Huang et al., 2014a), no a robust method of performing direct and precise $PM_{2.5}$ source

apportionment exists due to the complexity of the emission sources and atmospheric processes. Carbonaceous aerosols are not only the most important fractions of $PM_{2.5}$, but also the main factors that significantly lead to severe air pollution and deterioration in atmospheric visibility (Cao et al., 2003; Cao et al., 2007; Deng et al., 2008; Yang et al., 2011) owing to their strong ability for scattering and absorbing visible light (Bond et al., 2006; Kanakidou et al., 2005). Source apportionment based on ^{14}C analysis has the potential to unambiguously separate the various carbon species into fossil (^{14}C-free) and non-fossil fractions (modern ^{14}C level) (Gustafsson et al., 2009; Huang et al., 2014a; Kirillova et al., 2013; Liu et al., 2013b; Szidat et al., 2004; Weber et al., 2007; Wozniak et al., 2012; Lewis et al., 2004), providing significant information on the $PM_{2.5}$ sources and corresponding atmospheric processes that they have undergone. Our results show that non-fossil emissions represent a significant portion of the TC in both North and South China: 56±4% in BJ and 46±5% in GZ, respectively (Table 2). Similar to previous studies conducted in cities around the world (Andersson et al., 2015; Bernardoni et al., 2013; Liu et al., 2013b; Szidat et al., 2009), EC is derived mainly from fossil-fuel combustion in urban regions. In the remote areas, biomass burning plays a more role in EC loading. Fox example, ~50-70% of EC were found come from the burning of biomass materials in Arctic (Barrett et al. 2015) and the nature protection area of China (Zhang et al. 2014). On average, a larger proportion of biomass burning in the EC in BJ (33±7%) relative to GZ (20±5%) indicates that the emissions of biomass burning, e.g., biofuel burning and outdoor fires in North China, are higher than those in South China. This result is consistent with the other observations in this study: the mean concentrations of Lev and K^+ in BJ are higher than in GZ by factors of 1.4 and 1.7, respectively (Table 1). More than half of the OC fraction is contributed by non-fossil sources in both BJ (59±4%) and GZ (54±6%). Although the ^{14}C levels in the OC in BJ and GZ have similar ranges, the cities differ considerably in the species of WIOC and WSOC. On average, the percentage of non-fossil carbon in WIOC in BJ (74±8%) is 23% higher than that in GZ (51±2%). This result is probably explained by the large

difference between North and South China in the types of biomass burned. In Beijing and its adjacent regions, annual plants, e.g., crop residues and agricultural grass, are the main materials involved in biomass burning activities (Cheng et al., 2013; Duan et al., 2004; Li et al., 2008; Li et al., 2010; Yan et al., 2006), Whereas, 2000 km south from BJ, in GZ, the types of biomass are marked by hardwood (Liu et al., 2014), which is further confirmed by the compositions of anhydrosugars in this study (Fig. S3). Compared to the hardwood burning (WIOC/OC = 79%), OC aerosols emitted directly from combustion of annual plants appeared to be more enriched in WIOC species (WIOC/OC = 97%) (Iinuma et al., 2007), which is probably the most important factor in the markedly higher ^{14}C levels in WIOC in BJ compared to those in GZ. In contrast, WSOC in BJ is more depleted in ^{14}C than that in GZ: 46±13% of WSOC in BJ and 60±11% in GZ is directly correlated with non-fossil sources. WSOC is regarded as a mixture of mainly SOC and POC_{bb} (Ding et al., 2008; Weber et al., 2007). Such a difference in the WSOC-^{14}C levels between the two cities could be attributed mainly to the origins and formation processes of the SOC, of which will be discussed below.

3.3 Source Apportionment

A source apportionment model for carbonaceous aerosols using the combined measurements of ^{14}C and biomass burning tracers was recently reported (Liu et al., 2014). Detailed information with respect to this model provided in the Methodology section of the paper. Significantly distinct characteristics between BJ and GZ are observed for the source apportionments of TC (Fig. 3). The largest contributor to TC in BJ is SOC_{nf} (28±2%), followed by SOC_f (26±5%), POC_{bb} (24±1%), POC_f (10±4%), EC_f (8±2%), and EC_{bb} (4±1%), whereas in GZ, an order of SOC_{nf} (31±2%) > POC_f (22±4%) > EC_f (18±3%) > SOC_f (15±9%) > POC_{bb} (10±4%) > EC_{bb} (4±1%) is observed. Consequently, the fraction of primary sources, i.e., the sum of POC and EC, was higher in GZ (54±9%) than that in BJ (46±4%). The variability of the source

apportionment results represent the 1σ standard deviation of the individual sources during the study. It should be noted that model uncertainties of the contributors mainly depend on correction factors such as $(POC/Lev)_{bb}$ emission ratios of wood-burning markers and conversion factors for determination of the fraction of contemporary carbon from ^{14}C analysis. Typical relative model uncertainties were recently estimated by Zhang et al. (2015) using a similar model approach as 20-25% for SOC_{nf}, SOC_f, POC_{bb}, and POC_f as well as ~13% for EC_f, and EC_{bb}.

POC and EC aerosols are independent of the conditions of atmospheric gas reactions and thus can directly reflect the characteristics of local emission sources. The total proportions of EC_f and POC_f in GZ (40±6%) are significantly higher than those in BJ (19±5%), indicating high emissions from fossil-fuel combustion in GZ. The ratios of POC_f to EC_f are similar in both cities: 1.3±0.42 in BJ and 1.2±0.26 in GZ. These fossil fuel-derived POC/EC ratios in ambient air are considerably lower than the ratios directly derived from industrial coal combustion (2.7-6.1) (Zhang et al., 2008) but close to those of traffic exhaust (0.5-1.3) (He et al., 2008; Zhou et al., 2014). The total proportions of EC_{bb} and POC_{bb} in the TC accounted for 28±1% and 15±5% in BJ and GZ, respectively, which confirmed the greater impact of biomass burning on regional air pollution in North China.

Of SOC, 52±5% and 71±11% are derived from non-fossil sources in BJ and GZ, respectively. Using multi-technique integrated methods, Huang et al. (2014a) found that 35-54% and 65-85% of the SOC were derived from non-fossil sources in BJ and GZ, respectively, which is consistent with our results. These findings underline the importance of the non-fossil contribution to SOC formation in China's megacities. The considerable difference in SOC composition between the two cities might be due to the significant difference in SOC precursors and corresponding atmospheric reaction processes. In spring (from March to early April), in North China, the land is bare and trees still leafless, whereas, in South China there is lush vegetation, which release non-fossil VOCs (isoprene, α-pinene, β-caryophyllene, etc.), which are SOC

precursors. Additionally, a close relationship is observed between POC_{bb} and SOC_{nf} in BJ ($R^2 = 0.99$) but not in GZ ($R^2 = 0.50$) (Fig. 2), indicating the predominant role of biomass burning-derived VOCs in SOC_{nf} formation in North China. Combined with the fact that the total proportion of EC_{bb} and POC_{bb} in TC in BJ is almost twofold higher than that in GZ, efforts to control biomass burning, such as fugitive open fires, burning of agricultural residue, and domestic cooking/heating, are likely the most means of mitigating haze pollution in the North China region. In addition to the difference in the SOC precursors, the difference in meteorological conditions between the two cities is another likely reason for the difference in SOC composition. Compared to fossil-derived SOC, non-fossil SOC would preferentially formed in a higher humidity environment (Liu et al., 2014; Favez et al., 2008). The relative humidity in GZ (79%, 66-95%) is much higher than that in BJ (48%, 19-79%) during the sampling campaign.

3.4 Source Dynamics of Carbonaceous Aerosols during Haze Process

Particulate-derived haze pollution is characterized by an elevated $PM_{2.5}$ mass concentration due to the rapid physical accumulation and intensive atmospheric reactions. Knowledge of the source dynamics of the fine particles is crucial to understanding haze pollution.

An integrated haze process is observed in GZ from Apr.11–17 (Fig. S4). From Apr. 11 (65 μg/m^3), the $PM_{2.5}$ concentration increases sharply at an average rate of 34 μg/m^3/day for two days, then reaches a plateau from Apr. 13-15 (132-145 μg/m^3), and fall sharply to 76 μg/m^3 on Apr. 17 at a rate of 35 μg/m^3/day. To illustrate this haze bloom-decay process, all component concentrations (C) are normalized to the concentration on the first day (C_o). The concentrations for these components are listed in Table S1. As shown in Fig. 4C, both total primary and secondary matter concentrations increase by a factor of ~1.5 from the first day to the second day (blooming stage), indicating that direct emissions and atmospheric reactions played the similar roles in $PM_{2.5}$ growth during this phase. Notably, primary fossil organic matter (POM_f),

335 EC_f and NO_3^- have the highest formation rates, with the values of $C/C_o > 2.0$ (Fig. 4A, B), implying greater
336 contribution of vehicle exhaust to the fine particles since NO_3^- is an indicator of traffic emissions. At the
337 haze outburst (the third day also the initial day of haze), the growth rates of total primary and secondary
338 matter diverge significantly, and the C/C_o values are 1.6 and 2.6, respectively, suggesting that atmospheric
339 reactions started to play a more important role in the particle growth than direct emission-derived particles.
340 The growth of POM_f, EC_f, secondary fossil organic matter (SOM_f) and NO_3^- ($C/C_o > 3.0$) are more rapid
341 than that of the other components, again indicating the important role of vehicle emissions. On the last day
342 of the haze episode, all primary matter C/C_o values markedly decrease, with the exception of unidentified
343 materials. This phenomenon could be explained by the rapid shift in the pollutant sources transported by
344 the air masses. As shown in Fig.1, air masses collected at the fifth day originated from southern GZ, a major
345 area of anthropogenic pollutant emission (Zheng et al., 2009) incorporating large-scale industry city
346 districts, such as Foshan, Zhongshan and Dongguan. These industry-derived air masses are likely enriched
347 with those materials that are not identified in this study, such as mineral dust. Furthermore, the C/C_o values
348 for industry-related secondary matter such as SO_4^{2-} (an indicator for industrial emissions) and SOM_f showed
349 a clear increase on the same day. The reason for the decline in the C/C_o values of SOM_{nf} is probably due to
350 the dilution of biogenic/biomass burning VOCs with the invasion of these industry-related air masses. All
351 of the C/C_o values of the secondary aerosols decrease markedly on the seventh day (Fig. 4A, B), indicating
352 that the atmospheric reactions has weakened in the post-haze phase, due in part to the scavenging effect of
353 the precipitation that occurred on Apr. 16 on the aged aerosols (Fig. S1).

354 In BJ, $PM_{2.5}$ concentrations remain high during the sampling period, and no clear bloom/decay haze
355 process similar to that observed in GZ is captured. It should be noted, however, that samples for the ^{14}C
356 measurements are not collected on consecutive days in BJ, as is case for GZ. Therefore, C/C_o values are
357 plotted in Fig. 4 along the increasing trend of $PM_{2.5}$ concentrations. After comparing the characteristics of

relative lower and higher $PM_{2.5}$ loadings, a recent study revealed that severe haze pollution in North China is controlled by the secondary matters (Huang et al., 2014a). Our results confirm this conclusion and find an anomalous relationship between $PM_{2.5}$ level and secondary matter (Fig. 4F), pointing out that atmospheric reactivity is not sufficient for the initiation of strong haze events. To a large extent, $PM_{2.5}$ and secondary aerosols in North China is depending on meteorological conditions and the origins of air masses (Guo et al., 2014). $PM_{2.5}$ pollution on Mar. 25 is more severe than that on Mar.16, while the C/C_o of total secondary matter Mar. 16 is much higher than Mar. 25 (Fig. 4F). Most air masses reaching on Mar.16 come from the most polluted region in North China, i.e. southern BJ (Fig. 1 and Fig. S2). These migrated aerosols would underwent lots of atmospheric reactions and aged process. On other hand, NO_3^- displays the highest growth rate among all of the types of matter, indicating that traffic emissions contribute most to the air pollution. However, SOM_{nf}, which in this study is mostly derived from biomass burning (section 3.3), plays a more important role than SOM_f (Fig. 4E), implying the importance of biomass burning in haze formation in BJ. This is much different from that in South China (Fig. 4B). Furthermore, the NH_4^+ C/C_o along the increase of $PM_{2.5}$ loading in BJ is ~5-10 times as high as that in GZ. This is probably because North China, especially those regions in southern BJ (Heibei, Henan and Shandong), has the most intensive NH_4^+ emissions from fertilizer and livestock in China (Huang et al., 2012; Zhang et al., 2010b). In addition, it is reported that the emission factor of NH_4^+ from annual plant burning (47 mg/kg) is found to be approximately fivefold that of hardwood burning (10 mg/kg) (Iinuma et al., 2007). Therefore, the much higher NH_4^+ growth rate in BJ compared to that of GZ may partly be attributed to the importance of agricultural residue burning in the North China.

4 Conclusions

Severely high loadings of carbonaceous aerosols (CAs) regarding the deterioration of air quality, risk of

human health, and abnormal change of climate system in Chinese megacities has drawn a lot of scientific and public attentions. Through the combined measurements of powerful sources tracers (radiocarbon and anhydrosugars), this study reveals the significant differences of the origins of various CAs in the megacities of North (Beijing) and South China (Guangzhou). The contribution of non-fossil sources (e.g., domestic heating and cooking) to total carbon (TC), organic carbon (OC), water-soluble OC (WSOC), water-insoluble OC (WIOC), and elemental carbon (EC) is 56±4%, 59±4%, 46±13%, 74±8%, and 33±7% in Beijing, and 46±5%, 54±6%, 60±11%, 51±2%, and 20±5% in Guangzhou, respectively. Overall, non-fossil sources play a more important role in CAs in North China than South China. Lower contribution of non-fossil sources to secondary OC in Beijing than Guangzhou is largely because the much lower humidity and limited biogenic volatile organic compounds in North China during the sampling campaign. The air pollution controls in China probably should be enacted and performed according to the local circumstances. Finally, we find that primary aerosols play an equal important role on the haze blooming phase as secondary aerosols in South China, yet nitrate and fossil secondary organic matter predominate in the haze stage.

Acknowledgements. This research was supported by the "Strategic Priority Research Program (B)" of the Chinese Academy of Sciences (Grant No. XDB05040503), the Natural Science Foundation of China (NSFC; No.41430645 and 41473101), the State Key Laboratory of Organic Geochemistry Fund (No. SKLOG2013A01), and the Guangzhou Elites Scholarship Council (JY201332). The authors gratefully acknowledge the NOAA Air Resources Laboratory (ARL) for the provision of the HYSPLIT transport and dispersion mode. We also gratefully acknowledge the MODIS mission scientists and associated NASA personnel for the production of AOD data.

References

Andrews, E., Saxena, P., Musarra, S., Hildemann, L.M., Koutrakis, P., McMurry, P., Olmez, I. and White, W.H.: Concentration and composition of atmospheric aerosols from the 1995 SEAVS experiment and a review of the closure between chemical and gravimetric measurements. Journal of the Air & Waste Management Association, 50, 648-664, 2000.

Andersson, A., Deng, J., Du, K., Zheng, M., Yan, C., Sköld, M., and Gustafsson, Ö.: Regionally-varying combustion sources of the January 2013 severe haze events over eastern China. Environmental Science & Technology, 49, 2038-2043, 2015.

Barrett, T. E., Robinson, E. M., Usenko, S., and Sheesley, R. J.: Source contributions to wintertime elemental and organic carbon in the western arctic based on radiocarbon and tracer apportionment. Environmental Science & Technology, 49, 11631-11639, 2015.

Bernardoni, V., Calzolai, G., Chiari, M., Fedi, M., Lucarelli, F., Nava, S., Piazzalunga, A., Riccobono, F., Taccetti, F., and Valli, G.: Radiocarbon analysis on organic and elemental carbon in aerosol samples and source apportionment at an urban site in Northern Italy. Journal of Aerosol Science, 56, 88-99, 2013.

Bond, T. C. and Bergstrom, R. W., Light absorption by carbonaceous particles: An investigative review. Aerosol Science and Technology, 40, 27-67, 2006.

Brunekreef, B. and Holgate, S. T., Air pollution and health. The lancet, 360, 1233-1242, 2002.

Cao, J., Lee, S., Ho, K., Zhang, X., Zou, S., Fung, K., Chow, J. C., and Watson, J. G.: Characteristics of carbonaceous aerosol in Pearl River Delta Region, China during 2001 winter period. Atmospheric Environment, 37, 1451-1460, 2003.

Cao, J., Lee, S., Chow, J. C., Watson, J. G., Ho, K., Zhang, R., Jin, Z., Shen, Z., Chen, G., Kang, Y., Zou, S., Zhang, L., Qi, S., Dai, M., Cheng, Y., and Hu, K.: Spatial and seasonal distributions of carbonaceous aerosols over China. Journal of Geophysical Research: Atmospheres, 112, (D22), 2007

Cao, J.-J., Shen, Z.-X., Chow, J. C., Watson, J. G., Lee, S.-C., Tie, X.-X., Ho, K.-F., Wang, G.-H., and Han, Y.-M.: Winter and summer PM2.5 chemical compositions in fourteen Chinese cities. Journal of the Air & Waste Management Association 62, 1214-1226, 2012.

Chan, C. K. and Yao, X.: Air pollution in mega cities in China. Atmospheric Environment 42, 1-42, 2008.

Chen, B., Andersson, A., Lee, M., Kirillova, E. N., Xiao, Q., Kruså, M., Shi, M., Hu, K., Lu, Z., Streets, D. G., Du, K., and Gustafsson, Ö.: Source forensics of black carbon aerosols from China. Environmental Science & Technology, 47, 9102-9108, 2013.

Chen, J., Qiu, S., Shang, J., Wilfrid, O.M., Liu, X., Tian, H. and Boman, J.: Impact of relative humidity and water soluble constituents of PM2.5 on visibility impairment in Beijing, China. Aerosol and Air Quallity Research, 14, 260-268, 2014.

Chen, K.S., Lin, C.F. and Chou, Y.M.: Determination of source contributions to ambient PM2.5 in Kaohsiung, Taiwan, using a receptor model. Journal of the Air & Waste Management Association, 51, 489-498, 2001.

Cheng, Y., Engling, G., He, K.-B., Duan, F.-K., Ma, Y.-L., Du, Z.-Y., Liu, J.-M., Zheng, M., and Weber, R. J.: Biomass burning contribution to Beijing aerosol. Atmospheric Chemistry and Physics, 13, 7765-7781, 2013.

Chow, J.C., and Watson, J.G.: PM2.5 carbonate concentrations at regionally representative Interagency Monitoring of Protected Visual Environments sites, Joural of Geophysical Research: Atmospheres, 107, D21, 2002.

Dai, S., Bi, X., Chan, L.Y., He, J. Wang, B. Wang, X. Peng, P. Sheng, G., and Fu, J.: Chemical and stable carbon isotopic composition of $PM_{2.5}$ from on-road vehicle emissions in the PRD region and implications for vehicle emission control policy. Atmospheric Chemistry and Physics, 15, 3097-3108, 2015.

Deng, X., Tie, X., Wu, D., Zhou, X., Bi, X., Tan, H., Li, F., and Jiang, C.: Long-term trend of visibility and its characterizations in the Pearl River Delta (PRD) region, China. Atmospheric Environment 2008, 42, (7), 1424-1435.

Ding, X., Zheng, M., Yu, L., Zhang, X., Weber, R. J., Yan, B., Russell, A. G., Edgerton, E. S., and Wang, X.: Spatial and seasonal trends in biogenic secondary organic aerosol tracers and water-soluble organic carbon in the southeastern United States. Environmental Science & Technology, 42, 5171-5176, 2008.

Dockery, D. W., Pope, C. A., Xu, X., Spengler, J. D., Ware, J. H., Fay, M. E., Ferris Jr, B. G., and Speizer, F. E.: An association between air pollution and mortality in six US cities. New England Journal of Medicine, 329, 1753-1759, 1993.

Duan, F., Liu, X., Yu, T., and Cachier, H.: Identification and estimate of biomass burning contribution to the urban aerosol organic

carbon concentrations in Beijing. Atmospheric Environment, 38, 1275-1282, 2004.
Favez, O., Sciare, J., Cachier, H., Alfaro, S. C., and Abdelwahab, M. M.: Significant formation of water-insoluble secondary organic aerosols in semi-arid urban environment. Geophysical Research Letters, 35, L15801, 2008.
Favez, O., Cachier, H., Sciare, J., Sarda-Estève, R. and Martinon, L..: Evidence for a significant contribution of wood burning aerosols to $PM_{2.5}$ during the winter season in Paris, France. Atmospheric Environment, 43, 3640-3644, 2009.
Fine, P. M., Cass, G. R., and Simoneit, B. R.: Chemical characterization of fine particle emissions from the fireplace combustion of woods grown in the southern United States. Environmental Science & Technology, 36, 1442-1451, 2002.
Guo, S., Hu, M., Guo, Q., Zhang, X., Zheng, M., Zheng, J., Chang, C. C., Schauer, J. J., and Zhang, R.: Primary sources and secondary formation of organic aerosols in Beijing, China. Environmental Science & Technology, 46, 9846-9853, 2012.
Guo, S., Hu, M. Zamora, M. Peng, J. Shang, D., Zheng, J. Du, Z., Wu, Z., Shao, M., Zeng, L., Molina, M.J., and Zhang, R.: Elucidating severe urban haze formation in China. Proceedings of the National Academy of Sciences of the United States of America, 111, 17373-17378.
Gustafsson, Ö., Kruså, M., Zencak, Z., Sheesley, R. J., Granat, L., Engström, E., Praveen, P., Rao, P., Leck, C., and Rodhe, H.: Brown clouds over South Asia: biomass or fossil fuel combustion? Science, 323, 495-498, 2009.
He, H., Wang, Y., Ma, Q., Ma, J., Chu, B., Ji, D., Tang, G., Liu, C., Zhang, H., and Hao, J.: Mineral dust and NOx promote the conversion of SO_2 to sulfate in heavy pollution days. Scientific Reports, 4, 2014.
He, K., Yang, F., Ma, Y., Zhang, Q., Yao, X., Chan, C. K., Cadle, S., Chan, T., and Mulawa, P.: The characteristics of PM2.5 in Beijing, China. Atmospheric Environment, 35, 4959-4970, 2001.
He, L.-Y., Hu, M., Zhang, Y.-H., Huang, X.-F., and Yao, T.-T.: Fine particle emissions from on-road vehicles in the Zhujiang Tunnel, China. Environmental Science & Technology, 42, 4461-4466, 2008.
Hennigan, C. J., Sullivan, A. P., Collett, J. L., and Robinson, A. L.: Levoglucosan stability in biomass burning particles exposed to hydroxyl radicals. Geophysical Research Letters, 37, L09806, 2010.
Hoffmann, D., Tilgner, A., Iinuma, Y., and Herrmann, H.: Atmospheric stability of levoglucosan: a detailed laboratory and modeling study. Environmental Science & Technology, 44, 694-699, 2009.
Huang, J., Kang, S., Shen, C., Cong, Z., Liu, K., Wang, W. and Liu, L.: Seasonal variations and sources of ambient fossil and biogenic-derived carbonaceous aerosols based on ^{14}C measurements in Lhasa, Tibet. Atmospehric Research, 96, 553-559, 2010.
Huang, X., Song, Y., Li, M., Li, J., Huo, Q, Cai, X., Zhu, T., Hu, M., and Zhang H.: A high-resolution ammonia emission iventory in China. Global Biogeochemcial Cycles, 26, GB1030, 2012.
Huang, R.-J., Zhang, Y., Bozzetti, C., Ho, K.-F., Cao, J.-J., Han, Y., Daellenbach, K. R., Slowik, J. G., Platt, S. M., Canonaco, F., Zotter, P., Wolf, R., Pieber, S. M., Bruns, E. A., Crippa, M., Ciarelli, G., Piazzalunga, A., Schwikowski, M., Abbaszade, G., Schnelle-Kreis, J., Ralf, Z., An, Z., Szidat, S., Baltensperger, U., Haddad, I. E., and Prévôt, A.S.H.: High secondary aerosol contribution to particulate pollution during haze events in China. Nature, 514, 218-222, 2014a.
Huang, Y., Shen, H., Chen, H., Wang, R., Zhang, Y., Su, S., Chen, Y., Lin, N., Zhuo, S., Zhong, Q., Wang, X., Liu, J., Li, B., Liu, W., and Tao, S.: Quantification of Global Primary Emissions of PM2.5, PM10, and TSP from Combustion and Industrial Process Sources. Environmental Science & Technology, 48, 13834-13843, 2014b.
Iinuma, Y., Brüggemann, E., Gnauk, T., Müller, K., Andreae, M., Helas, G., Parmar, R., and Herrmann, H.: Source characterization of biomass burning particles: The combustion of selected European conifers, African hardwood, savanna grass, and German and Indonesian peat. Journal of Geophysical Research: Atmospheres, 112, D08209, 2007.
Kanakidou, M., Seinfeld, J., Pandis, S., Barnes, I., Dentener, F., Facchini, M., Dingenen, R. V., Ervens, B., Nenes, A., Nielsen, C., Swietlicki, E., Putaud, J., Balkanski, Y., Fuzzi, S., Horth, J., Moortgat, G., Winterhalter, R., Myhre, C., Tsigaridis, K., Vignati, E., Stephanou, E., and Wilson, J.: Organic aerosol and global climate modelling: a review. Atmospheric Chemistry and Physics, 5, 1053-1123, 2005
Kirillova, E. N., Andersson, A., Sheesley, R. J., Kruså, M., Praveen, P., Budhavant, K., Safai, P., Rao, P., and Gustafsson, Ö.: 13C-and 14C-based study of sources and atmospheric processing of water-soluble organic carbon (WSOC) in South Asian aerosols. Journal of Geophysical Research: Atmospheres, 118, 614-626, 2013

Lewis, C. W., Klouda, G. A., and Ellenson, W. D.: Radiocarbon measurement of the biogenic contribution to summertime PM2.5 ambient aerosol in Nashville, TN. Atmospheric Environment, 38, 6053-6061, 2004.

Li, L., Wang, Y., Zhang, Q., Li, J., Yang, X., and Jin, J.: Wheat straw burning and its associated impacts on Beijing air quality. Science in China Series D: Earth Sciences, 51, 403-414, 2008.

Li, W., Shao, L., and Buseck, P.: Haze types in Beijing and the influence of agricultural biomass burning. Atmospheric Chemistry and Physics, 10, 8119-8130, 2010.

Lim, S. S., Vos, T., Flaxman, A. D., Danaei, G., Shibuya, K., Adair-Rohani, H., AlMazroa, M. A., Amann, M., Anderson, H. R., Andrews, K. G., Aryee, M., Atkinson, C., Bacchus, L. J., Bahalim, A. N., Balakrishnan, K., Balmes, J., Barker-Collo, S., Baxter, A., Bell, M. L., and Blore, J. D.: A comparative risk assessment of burden of disease and injury attributable to 67 risk factors and risk factor clusters in 21 regions, 1990–2010: a systematic analysis for the Global Burden of Disease Study 2010. The lancet, 380, 2224-2260, 2013.

Liu, X., Li, J., Qu, Y., Han, T., Hou, L., Gu, J., Chen, C., Yang, Y., Liu, X., Yang, T., Zhang, Y., Tian, H., and Hu, M.: Formation and evolution mechanism of regional haze: a case study in the megacity Beijing, China. Atmospheric Chemistry and Physics, 13, 4501-4514, 2013a.

Liu, D., Li, J., Zhang, Y., Xu, Y., Liu, X., Ding, P., Shen, C., Chen, Y., Tian, C., and Zhang, G.: The use of levoglucosan and radiocarbon for source apportionment of PM2.5 carbonaceous aerosols at a background site in East China. Environmental Science & Technology, 47, 10454-10461, 2013b.

Liu, J., Li, J., Zhang, Y., Liu, D., Ding, P., Shen, C., Shen, K., He, Q., Ding, X., Wang, X., Chen, D., Szidat, S., and Zhang, G.: Source Apportionment Using Radiocarbon and Organic Tracers for PM2.5 Carbonaceous Aerosols in Guangzhou, South China: Contrasting Local-and Regional-Scale Haze Events. Environmental Science & Technology, 48, 12002-12011, 2014.

Liu, S., Tao, S., Liu, W., Liu, Y., Dou, H., Zhao, J., Wang, L., Wang, J., Tian, Z., and Gao, Y., Atmospheric polycyclic aromatic hydrocarbons in North China: a winter-time study. Environmental Science & Technology, 41, 8256-8261, 2007.

Miyazaki, Y., Kondo, Y., Takegawa, N. Komazaki, Y., Fukuda, M., Kawamura, K., Mochida, M., Okuzawa, K. and Weber, R.J.: Time-resolved measurements of water-soluble organic carbon in Tokyo. Journal of Geophysical Research: Atmospheres, 111, D23206, 2006

Mohn, J., Szidat, S., Fellner, J., Rechberger, H., Quartier, R., Buchmann, B., and Emmenegger, L.: Determination of biogenic and fossil CO_2 emitted by waste incineration based on $^{14}CO_2$ and mass balances, Bioresource Technol., 99, 6471-6479, doi:10.1016/j.biortech.2007.11.042, 2008.

Niu, Z., Wang, S., Chen, J., Zhang, F., Chen, X., He, C., Lin, L., Yin, L., and Xu, L.: Source contributions to carbonaceous species in PM2.5 and their uncertainty analysis at typical urban, peri-urban and background sites in southeast China. Environmental Pollution, 181, 107-114, 2013.

Simoneit, B. R. and Elias, V. O.: Detecting organic tracers from biomass burning in the atmosphere. Marine Pollution Bulletin, 42, 805-810, 2001.

Sun, Y., Zhang, Q., Zheng, M., Ding, X., Edgerton, E.S. and Wang, X.: Characterization and source apportionment of water-soluble organic matter in atmospheric fine particles ($PM_{2.5}$) with high-resolution aerosol mass spectrometry and GC–MS. Environmental Science & Technology, 45, 4854-4861, 2011.

Szidat, S., Jenk, T. M., Gäggeler, H. W., Synal, H.-A., Fisseha, R., Baltensperger, U., Kalberer, M., Samburova, V., Reimann, S., Kasper-Giebl, A., and Hajdas, I.: Radiocarbon (14C)-deduced biogenic and anthropogenic contributions to organic carbon (OC) of urban aerosols from Zürich, Switzerland. Atmospheric Environment, 38, 4035-4044, 2004.

Szidat, S., Ruff, M., Perron, N., Wacker, L., Synal, H.-A., Hallquist, M., Shannigrahi, A. S., Yttri, K., Dye, C., and Simpson, D.: Fossil and non-fossil sources of organic carbon (OC) and elemental carbon (EC) in Göteborg, Sweden. Atmospheric Chemistry and Physics, 9, 1521-1535, 2009.

Wang, Y., Wan, Q., Meng, W., Liao, F., Tan, H., and Zhang, R.: Long-term impacts of aerosols on precipitation and lightning over the Pearl River Delta megacity area in China. Atmospheric Chemistry and Physics, 11, 12421-12436, 2011.

Wang, Y., Wang, M., Zhang, R., Ghan, S. J., Lin, Y., Hu, J., Pan, B., Levy, M., Jiang, J. H., and Molina, M. J.: Assessing the effects of anthropogenic aerosols on Pacific storm track using a multiscale global climate model. Proceedings of the National Academy

of Sciences of the United States of America, 111, 6894-6899, 2014

Weber, R. J., Sullivan, A. P., Peltier, R. E., Russell, A., Yan, B., Zheng, M., De Gouw, J., Warneke, C., Brock, C., Holloway, J. S., Atlas, E. L., and Edgerton, E.: A study of secondary organic aerosol formation in the anthropogenic-influenced southeastern United States. Journal of Geophysical Research: Atmospheres, 112, D13302, 2007

Wozniak, A. S., Bauer, J. E., and Dickhut, R. M.: Characteristics of water-soluble organic carbon associated with aerosol particles in the eastern United States. Atmospheric Environment, 46, 181-188, 2012.

Yan, X., Ohara, T., and Akimoto, H.: Bottom-up estimate of biomass burning in mainland China. Atmospheric Environment, 40, 5262-5273, 2006.

Yang, F., He, K., Ye, B., Chen, X., Cha, L., Cadle, S.H., Chan, T., and Mulawa, P.A.: One-year record of organic and elemental carbon in fine particles in downtown Beijing and Shanghai. Atmopsheric Chemistry and Physics, 5, 1449-1457, 2005.

Yang, F., Tan, J., Zhao, Q., Du, Z., He, K., Ma, Y., Duan, F., Chen, G., and Zhao, Q.: Characteristics of PM2.5 speciation in representative megacities and across China. Atmospheirc Chemistry and Physics, 11, 5207-5219, 2011.

Yttri, K., Aas, W., Bjerke, A., Cape, J., Cavalli, F., Ceburnis, D., Dye, C., Emblico, L., Facchini, M., Forster, C., Hanssen, J., Hansson, H., Jennings, S., Maenhaut, W., Putaud, J., and Tørseth, K.: Elemental and organic carbon in PM10: a one year measurement campaign within the European Monitoring and Evaluation Programme EMEP. Atmospheric Chemistry and Physics, 7, 5711-5725, 2007.

Zhang, Q., He, K., and Huo, H.: Policy: cleaning China's air. Nature, 484, 161-162, 2012.

Zhang, Y., Liu, D., Shen, C., Ding, P., and Zhang, G.: Development of a preparation system for the radiocarbon analysis of organic carbon in carbonaceous aerosols in China. Nuclear Instruments and Methods in Physics Research Section B: Beam Interactions with Materials and Atoms, 268, 2831-2834, 2010a.

Zhang, Y. Dore, A.J., Ma, L., Liu, X.J., Ma, W.Q., Cape, J.N. and Zhang, F.S.: Agricultural amomonia emissions inventroy and spatial distribution in the North China Plain. Environmental Pollution, 158, 490-501, 2010b.

Zhang, Y.-L., Li, J., Zhang, G., Zotter, P., Huang, R.-J., Tang, J.-H., Wacker, L., Prévôt, A. S., and Szidat, S.: Radiocarbon-based source apportionment of carbonaceous aerosols at a regional background site on Hainan Island, South China. Environmental Science & Technology, 48, 2651-2659, 2014.

Zhang, Y.-L., Huang, R.-J., El Haddad, I., Ho, K.-F., Cao, J.-J., Han, Y., Zotter, P., Bozzetti, C., Daellenbach, K., Canonaco, F., Slowik, J., Salazar, G., Schwikowski, M., Schnelle-Kreis, J., Abbaszade, G., Zimmermann, R., Baltensperger, U., Prévôt, A., and Szidat, S.: Fossil vs. non-fossil sources of fine carbonaceous aerosols in four Chinese cities during the extreme winter haze episode of 2013. Atmospheric Chemistry and Physics, 15, 1299-1312, 2015.

Zhang, Y., Schauer, J. J., Zhang, Y., Zeng, L., Wei, Y., Liu, Y., and Shao, M.: Characteristics of particulate carbon emissions from real-world Chinese coal combustion. Environmental Science & Technology, 42, 5068-5073, 2008.

Zheng, J., Zhang, L., Che, W., Zheng, Z., and Yin, S.: A highly resolved temporal and spatial air pollutant emission inventory for the Pearl River Delta region, China and its uncertainty assessment. Atmospheric Environment, 43, 5112-5122, 2009.

Zheng, M., Salmon, L. G., Schauer, J. J., Zeng, L., Kiang, C., Zhang, Y., and Cass, G. R.: Seasonal trends in PM2.5 source contributions in Beijing, China. Atmospheric Environment, 39, 3967-3976, 2005.

Zhou, R., Wang, S., Shi, C., Wang, W., Zhao, H., Liu, R., Chen, L., and Zhou, B.: Study on the Traffic Air Pollution inside and outside a Road Tunnel in Shanghai, China. PloS one, 9, e112195, 2014.

580 Table 1 Dataset (average values with standard deviation) for the measured components in this study. Units

581 for the carbon fractions, anhydrosugars and ions are μg C/m^3, ng/m^3, μg/m^3, respectively.

	Beijing (North China) (Mar. 15 – Apr. 12, 2013)		Guangzhou (South China) (Apr. 04 – Apr. 18, 2013)	
	Average	Std.	Average	Std.
WIOC	9.07	4.88	5.99	3.37
WSOC	10.2	5.76	4.31	2.25
OC	19.2	10.3	10.3	5.13
EC	2.56	1.68	3.04	1.42
TC	21.8	11.9	13.3	6.47
Gal	11.7	7.78	5.75	2.51
Mann	10.3	6.24	11.5	5.47
Lev	369	249	259	172
Na^+	0.83	0.32	0.34	0.15
NH_4^+	13.0	10.6	7.01	3.05
K^+	1.43	0.90	0.82	0.34
Mg^{2+}	0.48	0.19	0.07	0.03
Ca^{2+}	5.63	2.54	0.60	0.36
Cl^-	5.62	3.30	1.91	1.68
NO_3^-	31.1	27.9	10.2	6.99
SO_4^{2-}	20.8	14.1	13.9	3.87

582 WIOC: water-insoluble organic carbon; WSOC: water-soluble organic carbon; OC: organic carbon; EC:

583 elemental carbon; TC: total carbon; Gal: galactosan; Mann: mannosan; Lev: levoglucosan;

584

585

586 Table 2 Percentages of non-fossil sources in various carbon species (%)

Location	Sampling Data	OC	WIOC	WSOC	EC	TC	SOC
Beijing (BJ, North China)	Mar.16	58±4	67±3	52±3	34±2	55±4	52±11
	Mar.22	54±5	83±4	53±3	33±2	60±5	55±11
	Mar.25	59±4	65±3	52±2	24±1	54±4	58±13
	Apr.10	54±4	82±4	22±1	43±2	53±4	43±11
	Average	59±4	74±8	46±13	33±7	56±4	52±5
Guangzhou (GZ, South China)	Apr.11	59±4	52±2	68±3	28±1	52±4	74±10
	Apr.12	53±4	50±2	60±3	21±1	46±4	77±10
	Apr.13	57±4	53±3	63±3	19±1	49±7	75±8
	Apr.15	42±3	48±2	39±2	18±1	38±3	49±5
	Apr.17	58±4	50±2	68±3	12±1	45±4	78±6
	Average	54±6	51±2	60±11	20±5	46±5	71±11

587

588

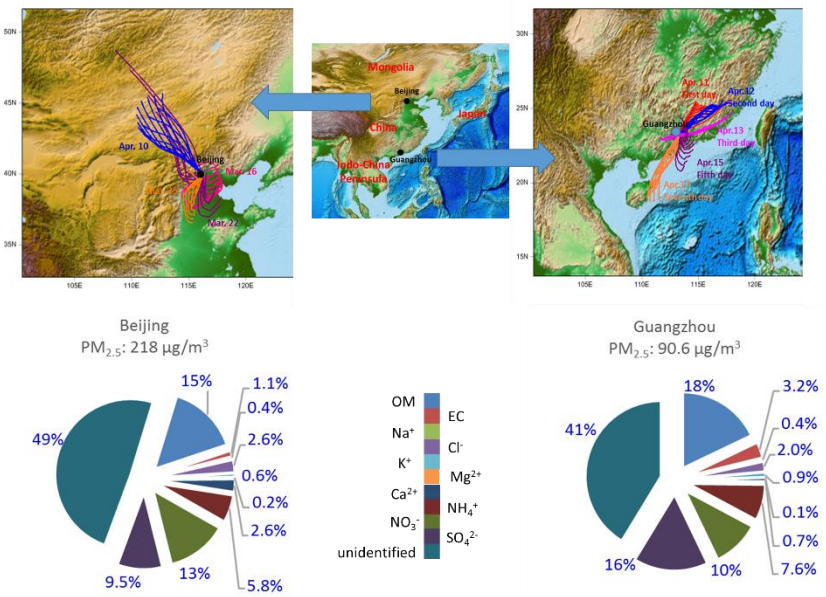

Fig. 1 Geographic locations of Beijing and Guangzhou as well as their $PM_{2.5}$ chemical compositions. Air mass back trajectories within 24 hours (run every 2 hours from the end of sampling) for the selected samples are modeled at 100 m above ground level by Air Resources Laboratory, National Oceanic and Atmospheric Administration (Hybrid Single Particle Lagrangian Integrated Trajectory Model).

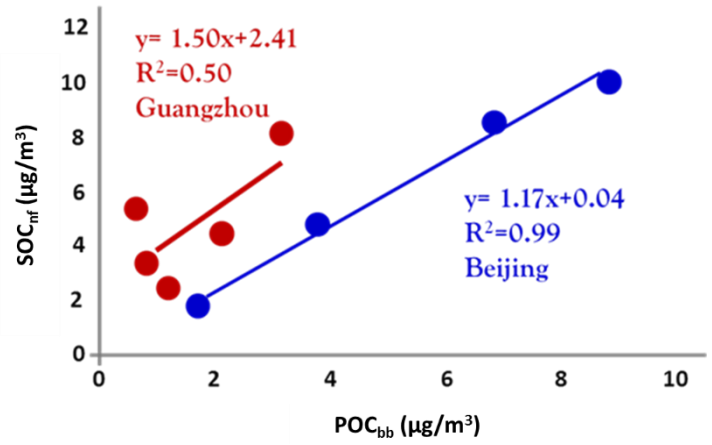

596

597 Fig.2 Correlations between the primary biomass burning OC (POC_{bb}) and the non-fossil secondary organic

598 carbon (SOC_{nf})

599

600

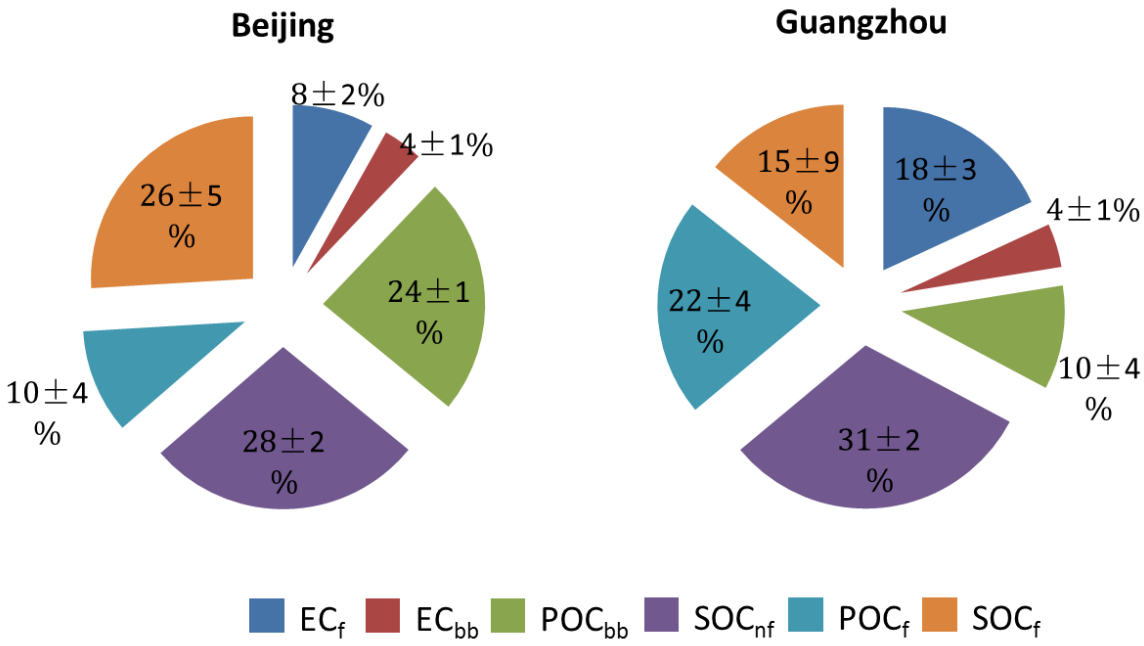

601

602 Fig.3 Relative contributions (%) of different carbon species to total carbon with variability of the

603 individual sources during the study. For model uncertainties of the individual fractions see Chapter 3.3.

604

605

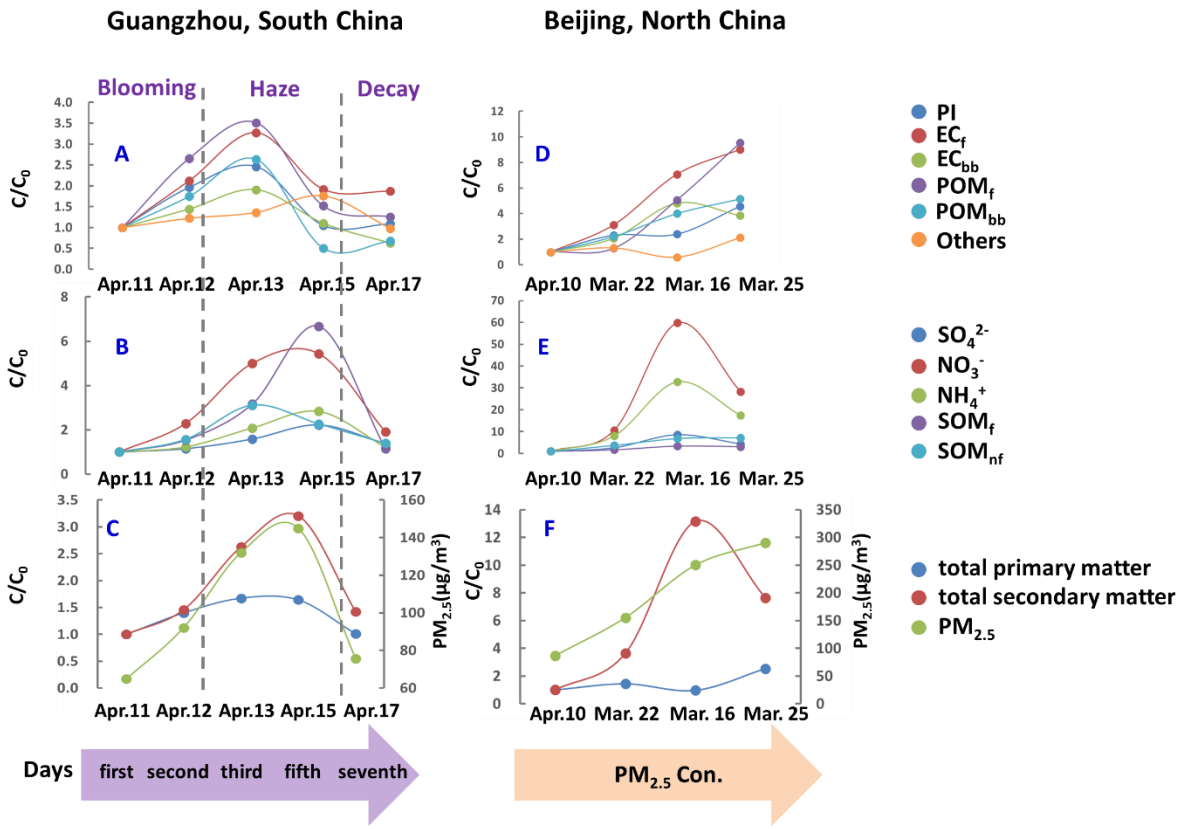

606

607 Fig.4 Dynamic changes for the primary and secondary matters in Chinese cities. Detailed concentrations
608 and the calculation methods are shown in Table S2. The first day is Apr. 11 in Guangzhou. For Beijing,
609 samples are ordered by their $PM_{2.5}$ concentrations. All concentrations (C) are normalized to that of a
610 reference day (C_o), i.e. the first day and the day with the lowest $PM_{2.5}$ concentration for Guangzhou and
611 Beijing, respectively. PI: primary ions; POM_f: primary fossil organic matter; POM_{bb}: biomass burning
612 organic matter; SOM_f: secondary fossil organic matter; SOM_{nf}: secondary non-fossil organic matter.